EFFECTS OF AEROSOLS ON THE OBSERVED IRRADIANCE FROM THE ULTRAVIOLET TO NEAR-INFRARED AT THE SURFACE OF MARS

J. P. Mason , **M.R Patel,** *PSSRI, The Open University, Milton Keynes, UK (j.p.mason@open.ac.uk)*, **S.R Lewis**, *Department of Physics & Astronomy, The Open University, Milton Keynes, UK*

Introduction:

Aeolian dust is the major climate driver component of the Martian atmosphere with variations in dust loading having significant effect on the atmospheric dynamics [1, 2]. So far there have been significant studies on Martian aeolian dust using observations from landers [3, 4], orbiting spacecraft [5, 6] and measurements from the Earth [7]. However, currently lacking is *in situ* information and characterization of the irradiance encountered at the surface of Mars in the UV, visible and NIR wavelengths and how different aerosols species influence the observed spectrum at the surface of Mars.

In this work, a radiative transfer model is used to simulate the irradiance observed at the surface of Mars in the 200 – 1100 nm region for different loadings of various aerosols species. Of interest is the modification of the spectrum and determining what information can be obtained about the aerosol species' single scattering properties. The aerosols considered in this analysis are, dust, water ice, CO_2 ice and water vapour covering the physical phenomenon of the background dust, dust clouds [8, 9], H_2O ice clouds [9, 10] , CO_2 ice clouds [11, 12] and near-surface morning fogs [13, 14].

Current models to determine the single scattering properties of Martian atmospheric dust from spectrum observations assume a uniform dust component within the modeled atmosphere (i.e. constant optical properties as a function of pressure). In reality this is not the case, with smaller particles being more prevalent in the upper atmosphere and larger particles being present closer to the surface. Differences in particle size will affect the single scattering properties of the dust, namely the extinction efficiency, single scattering albedo and asymmetry parameter. In this work the accuracy of the uniform dust assumption is investigated.

Radiative transfer models:

Two radiative transfer models were developed for this study into Martian aerosols. Both models are modified versions of the radiative transfer model, [15, 16, 17], which uses the delta-Eddington approximation to simulate the passage of solar radiation through the Martian atmosphere in the 200 - 1100 nm region. Within the model the atmosphere is divided into 70 separate layers corresponding to an altitude range of 0 to 140 km. The altitude resolution is a definable parameter, allowing increased altitude resolution for the surface fog and CO_2 ice cloud investigations.

For the aeolian dust analysis the Homogeneous Model (henceforth called HM) assumes a uniform dust component with the optical properties and particle size constant with pressure. The Vertical Model (henceforth called VM) employs a vertically varying dust component which scales the effective radius of the dust size distribution with pressure.

The variation of effective radius as a function of altitude was taken from [18] and provides three distributions for $r_{eff}(z)$ for different values of the effective variance which are held constant with altitude. The distributions only give values of $r_{eff}(z)$ up to 24 km, for altitudes greater than 24 km the effective radius is scaled with pressure until a particle size of 0.2 μm is reached, after which the dust component is assumed uniform. Figure 1 shows the resultant effective radius as a function of pressure and altitude.

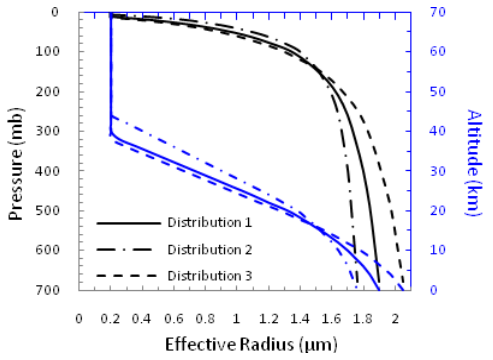

Figure 1: Dependence of the effective radius on pressure (black lines) and altitude (blue lines) for the three distributions given by [18].

The dust particle radii follow a log-normal distribution, though this is somewhat arbitrary since the effective radius and variance are used to describe the first and second moments of the distribution [19].

The single scattering dust properties are determined within the models by Mie scattering theory for spherical particles [19] or T-matrix code to simulate random orientated non-spherical particles. The ice cloud particle single scattering properties are calculated using a Mie scattering algorithm for coated spheres [19].

Martian Dust Investigations:

Irradiance sensitivity to dust properties. The total irradiance for different particle size distributions was produced using the HM to determine the sensitivity of the total irradiance to changes in (1) the effective radius and (2) the effective variance. For the first case the effective variance was held constant and the effective radius was given values of 1.0, 1.5, 2.0, 3.0 and 5.0 μm. For the second case the r_{eff} was held constant and v_{eff} was given the values 0.1, 0.2,

0.4, 0.8, and 1.0. Figure 2 shows the changes in the total irradiance for each case.

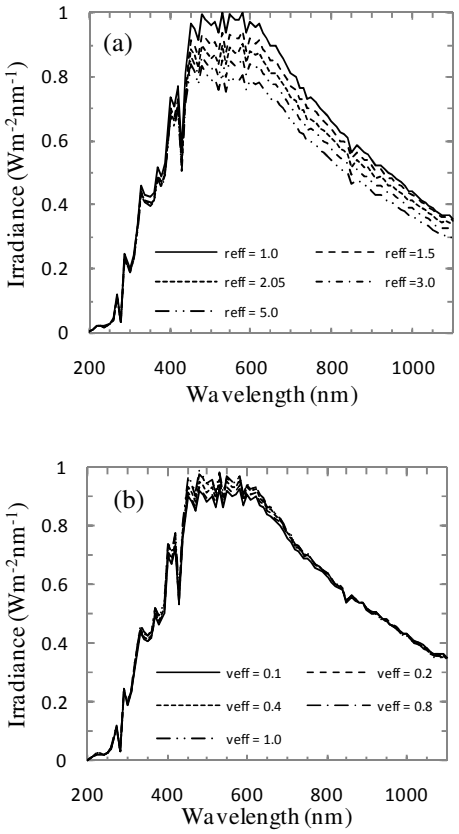

Figure 2: Changes in the total received irradiances for different values of (a) effective radius, (b) effective variance.

As the effective radius increases there is a decrease in the observed total irradiance from 450 nm to 1100 nm. This decrease is related to the scattering nature of the particles, as the particles become larger compared to the wavelength of interest they scatter more favorably in the forward direction thus reducing the amount of diffuse flux received at the surface. Interestingly, the total irradiance at wavelengths <450 nm is less sensitive to changes in the effective radius. This is explained by the reduced important of scattering at these wavelengths, were martian dust exhibits stronger absorption which is shown by the single scattering albedo and imaginary refractive index [20]. This result indicates that trying to determine the effective radius of the dust particle size distribution by attempting to fit a model spectrum to an observed spectrum within the wavelength region 180 – 450 nm would be extremely difficult. Fortunately above 450 nm the differences in total irradiance for different particle size distributions can be clearly seen. While size distributions with an effective radius value of 3.0 and 5.0 μm are extreme for suspended Martian dust, the difference in spectra between the more realistic values of r_{eff} (1.5 μm and 2.05 μm) is large enough in the wavelength region 450 to 800 nm to allow determination of different dust size distributions. For smaller particle sizes the difference in total irradiance becomes less obvious even at longer wavelengths, which reflects the reduced importance of the particle size relative to wavelength in scattering processes at small size parameters, ($2\pi R/\lambda$).

The sensitivity of the total observed irradiance to the dust particle's effective radius implies that the uniform dust assumption could be introducing errors into the simulated irradiances by having a larger value of r_{eff} at higher altitudes than would be realistically present as a result of sedimentation. As stated, the particle size affects its scattering properties, thus allowing r_{eff} to scale vertically with pressure would see smaller particle present at higher altitudes which will in turn have an impact on the received diffuse flux at the shorter wavelengths.

As illustrated in Figure 2 changes in the effective variance has little effect on the total received irradiance, there is negligible difference in the total flux for particle distributions with variances of 0.2 and 0.1. As the effective variance increases the difference with respect to the 0.1 case are greater, however, even at extreme variances (0.8 and 1.0) these differences only amount to difference of 7% within the 200- 600 nm wavelength region.

H_2O ice clouds: Previous investigations into Martian H_2O ice clouds have revealed significant variation in the derived size distribution for the cloud particles with the effective radius ranging from 0.5 μm [14], 1- 2 μm [6] and 3- 4 μm [21]. It has been hypothesized that these variations are a result of potentially different cloud types.

Pure ice particles. The first set of simulations makes the assumption a pure water ice particles existing with the cloud structure. A range of size distributions with r_{eff} = 0.5, 1.0, 3.0 and 4.0 μm were used to cover the range of potential different cloud types and the optical depth of the cloud was varied from 0.05 to 0.67. The simulated spectra are normalised to 800 nm to help emphasize the differences. Figure 3a shows for a cloud of low optical depth the attenuation of the observed irradiance spectrum is small, for higher optical depths, Figure 3b, the differences are more noticeable especially 400 – 700 nm wavelength range.

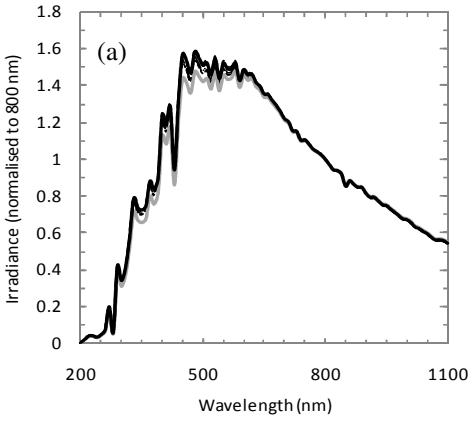

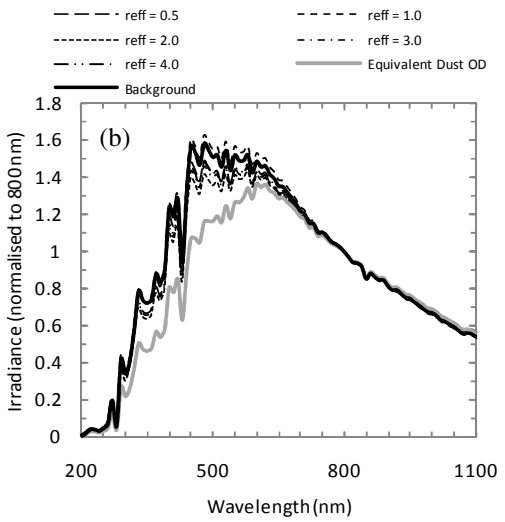

Figure 3: Attenuation of the total irradiance spectra for H_2O cloud optical depths of (a) 0.1 and (b) 0.45. The Legend in (b) is applicable to (a).

If the cloud feature is an isolated incident the ratio of the irradiance spectrum prior to the cloud encounter and during the encounter can be used to determine the transmission through the cloud, figure 4.

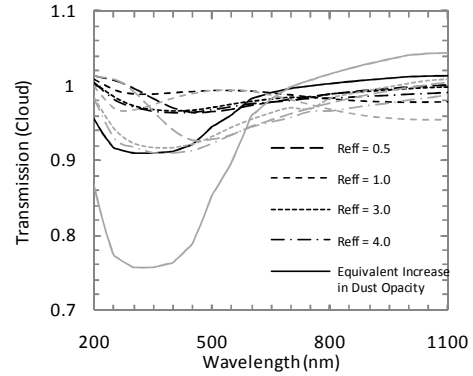

Figure 4: The transmission through the cloud for optical depths of 0.1 (black lines) and 0.45 (grey lines).

For clouds of low optical depth (0.1), little change is seen in the observed irradiances. For increasing optical depth the attenuation caused by the H_2O ice cloud is more noticeable especially for larger particle sizes (3-4 μm). Comparing to an equivalent increase in the dust optical depth (solid black and gray lines in figure 4) the characteristic absorption at bluer wavelength as a result of dust absorption is significantly reduced; this is a result of increased scattering by the ice particles at these wavelengths resulting in a higher diffuse flux. The increase in irradiance at redder wavelengths as a result of dust scattering is also reduced with little net increase observed in the presence of H_2O ice. This change in the attenuation of the incoming light could be used to indirectly infer the presence of a water ice cloud, however, as Figure 4 illustrates it would be difficult to deduce the particle size distribution and the optical properties of the cloud particles for low opacity clouds.

CO_2 ice clouds: The presence of CO_2 ice clouds at altitude >50 km have been observed by both orbiting spacecraft [11, 22] and anders [12], however, the conclusions and estimates of the cloud particles properties are far from definitive. The formation of CO_2 ice clouds is a result of atmospheric temperatures at high altitudes being low enough for to allow condensation of the CO_2 atmosphere [12].

The same technique for modeling H_2O ice cloud effects was used to model CO_2 ice clouds. CO_2 ice clouds, however, exist much higher in the Martian atmosphere (> 50 km) [11]. The cloud particles were chosen to have a size distribution with an effective radius of 0.2 [12], 1.0 and 1.5 μm [22] and an effective variance of 0.1 and consist of pure CO_2 [23]. The optical depth of the CO_2 ice cloud was chosen to be 0.1. The vertical extent of the cloud was 10 km at an altitude of 70 km. The ratio of the background irradiance compared to the irradiance during a CO_2 cloud event is shown in Figure 5. Also shown for comparison is the passage of a H_2O cloud with the same optical depth and various size distributions and the case for an equivalent increase in the dust background haze.

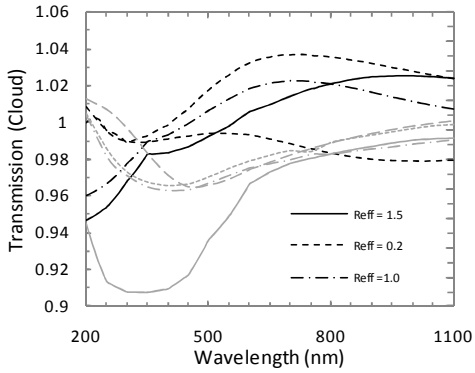

Figure 5: Transmission through CO2 ice clouds (black lines), H_2O ice clouds (gray lines, see figure 4 legend for details) and dust cloud (solid Gray line) for an optical depth of 0.1.

The attenuation caused by the CO_2 clouds is small, but the H_2O and CO_2 spectral signatures are quite different. The CO_2 clouds exhibit increased flux at all wavelengths > 350 nm. Below 350 nm there is a sharp decline in transmittance due to increased absorption by the CO_2 ice particles.

It should be noted that using Mie theory to calculate the single scattering properties of the CO_2 ice particles is far from accurate and the ice particles are likely to be cubic in nature [24]. However, since the opacities of the clouds are small and have little impact on the observed irradiance at the surface of Mars, the errors introduced by using Mie theory should be small.

Another method can be used to distinguish between dust, water ice clouds and CO_2 ice clouds,

provided direct and diffuse fluxes can be determined. The ratio of the diffuse and direct flux for different optical depths and a particle size distribution of 1.0 μm is shown in Figure 6.

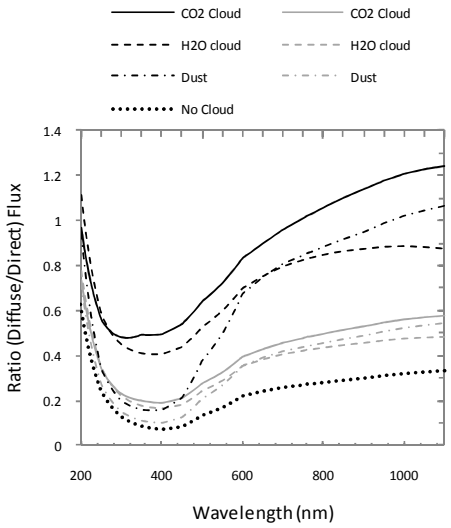

Figure 6: The diffuse / direct flux ratio for H_2O, CO_2 and dust clouds with an optical depth of 0.1 and 0.3. The effective radius was set to 1.0 μm for both cases.

The different cloud optical depths can be clearly seen as distinct offsets from the no cloud case. For low optical depths the observation of CO_2 ice clouds is difficult to distinguish from H_2O ice clouds with both showing very similar profiles, however, significant differences are seen when compared to a dust cloud event which has a much weaker diffuse flux at wavelengths <500 nm resulting from greater absorption at these wavelengths. At higher optical depths the CO_2 cloud departs from the H_2O cloud profile showing a higher ratio as a result of a higher diffuse flux. The result of the analysis into CO_2 ice clouds concludes that it would be extremely difficult to accurately determine the presence of CO_2 ice clouds from attenuation of surface irradiance spectra using the diffuse / direct flux ratio due to the similarity of its profile to H_2O ice clouds

Conclusions: The sensitivity of the total observed irradiance to the dust particle effective radius implies that the uniform dust assumption may introduce errors into the simulated irradiance. The resultant underestimation in the diffuse flux at shorter wavelengths as a result of large particles at higher altitudes could be of significant importance considering the low attenuation caused by the H_2O and CO_2 clouds and methods used for their detection.

It has been shown that the ratio of the diffuse and direct fluxes can be used to infer the presence of H_2O and CO_2 clouds from the background dust component; however, as shown in Figure 6 it would be difficult differentiate between the two cloud types as they both exhibit very similar profiles.

Future Work: The VM will be used to investigate the accuracy of the uniform dust assumption by scaling the surface effective radius with altitude and comparing the simulated irradiance components to those produced by the HM.

A fitting routine has been developed to extract the dust optical properties from irradiance spectra and will be used to determine the effective radius as seen by the HM model from the VM output irradiances.

The studies into H_2O and CO_2 clouds will be repeated using the VM and the observed irradiances and corresponding attenuation will be compared with the outputs produced by the HM using the retrieved size distribution from the fitting routine.

Acknowledgments:

This work is support by the UK Science and Technology Facilities Council (STFC).

References:

[1] Haberle, R.M., *et al.*, 1982, Icarus 50, 322-367. [2] Haberle, R.M., *et al.*, 1993, J. Geophys. Res 98, 3093-3123. [3] Smith, P.H. and M. Lemmon, 1999, J. Geophys. Res 104, 8975-8985. [4] Lemmon, M.T., *et al.* 2004, American Association for the Advancement of Science. p. 1753-1756. [5] Smith, M.D., 2008, [6] Clancy, R.T., *et al.*, 2003, J. Geophys. Res 108, [7] Wolff, M.J., *et al.*, 1999, J. Geophys. Res 104, [8] Cantor, B.A., *et al.*, 2001, J. Geophys. Res 106, 23653-23687. [9] Cantor, B., *et al.*, 2002, J. Geophys. Res 107, 5014. [10] Clancy, R.T. and S.W. Lee, 1991, Icarus 93, 135-158. [11] Montmessin, F., *et al.*, 2006, Icarus 183, 403-410. [12] Clancy, R.T. and B.J. Sandor, 1998, Geophysical Research Letters 25, 489-492. [13] Smith, P.H. and M. Lemmon, 1999, J. Geophys. Res 104, 8975–8985. [14] Petrova, E., *et al.*, 1996, Plan. Sp. Sci. 44, 1163-1176. [15] Otter, S., 2010, Thesis, Open University [16] Patel, M.R., *et al.*, 2002, Plan. Sp. Sci. 50, 915-927. [17] Patel, M.R., *et al.*, 2004, Icarus 168, 93-115. [18] Chassefière, E., *et al.*, 1995, J. Geophys. Res 100, 5525-5539. [19] Bohren, C.F. and D.R. Huffman, *Absorption and Scattering of Light by Small Particles*. 2004. [20] Ockert-Bell, M.E., *et al.*, 1997, J. Geophys. Res 102, 9039-9050. [21] Wolff, M.J. and R.T. Clancy, 2003, J. Geophys. Res 108, 5097. [22] Montmessin, F., *et al.*, 2007, J. Geophys. Res 112, E11S90. [23] Warren, S.G., 1986, Applied optics 25, 2650-2674. [24] Wergin, W.P., *et al.*, 2000, Microscopy and Microanalysis-New York 3, 1235-1236.